Available online at www.sciencedirect.com
SCIENCE DIRECT®
ELSEVIER
Earth and Planetary Science Letters 217 (2004) 379–388
EPSL
www.elsevier.com/locate/epsl

Tapping into the sub-seafloor: examining diffuse flow and temperature from an active seamount on the Juan de Fuca Ridge

Matthew J. Pruis *, H. Paul Johnson

School of Oceanography, University of Washington, Seattle, WA, USA

Received 16 January 2003; received in revised form 15 October 2003; accepted 17 October 2003

Abstract

A unique sampling strategy involving the cementing of a permanent fluid sampler directly to the seafloor on Axial Seamount, Juan de Fuca Ridge, has recently allowed the first long-term direct coupling to a low-temperature hydrothermal vent on a mid-ocean ridge. Using the hydrologically sealed sampler, direct measurement of fluid volume and heat flux from a diffuse hydrothermal vent on the seafloor was obtained over a period of 206 days. Enhanced variance at both tidal and lower frequencies was recorded with a high coherence between the temperature and flow data. We estimate a volume flux of 48 m^3/yr and a heat flux of 260 W/m^2 for the square meter of seafloor sampled by the instrument. Measurement of the Darcy flow velocities of the effluent fluid are approximately 1.5×10^{-6} m/s and indicate fluid velocities within cracks in the substrate of 1–4 m/day, with an effective upper crustal permeability of 10^{-11}–10^{-12} m^2. While the measured variability in fluid flow is driven primarily by changes in the thermal buoyancy of upwelling fluid, there is also a significant (above hydrostatic) pressure gradient contribution to the measured flux. This overpressure produces roughly four times the driving force compared to that attributed to thermal buoyancy alone. Small variations in the volume flux and the effluent fluid temperature ($\sim1.5\times10^{-8}$ m/s and ~0.5°C, respectively) also occurred on approximately tidal time scales and appear to be related to poroelastic control of the velocity of hydrothermal fluid through the seafloor boundary (i.e. tidal pumping).

Keywords: hydrothermal; hydrogeology; permeability; heat flow; tidal pumping

1. Introduction

Direct measurement of flow from diffuse hydrothermal systems has proven difficult because, unlike the visually impressive high-temperature edifices, diffuse flow is spread over a large spatial area and both the temperatures and the velocities of the fluid are small. The majority of previous studies have therefore focused on the measurement of diffuse fluxes utilizing integrative water column measurements [1–4]. These measurements allow efficient integration of the highly variable low-temperature fluxes over relatively large

* Corresponding author. Present address: NorthWest Research Associates, Inc., P.O. Box 3027, Bellevue, WA 98009-3027, USA. Tel.: +1-425-644-9660, ext. 311; Fax: +1-425-644-8422.
E-mail address: matt@nwra.com (M.J. Pruis).

0012-821X/03/$ – see front matter © 2003 Elsevier B.V. All rights reserved.
doi:10.1016/S0012-821X(03)00607-1

(vent-field scale) geographic areas, but are also complicated by the decoupled nature of the measurement and the source. Thus measurements of hydrothermal fluxes constrained to either the near-bottom boundary layer or the neutrally buoyant plume require careful analysis to separate effects from bottom currents, tidal flow and the natural spatial and temporal variability of diffuse plumes and their sources [5–8]. Even with these difficulties, these data have proven valuable in determining the partition between diffuse and high-temperature fluxes in mass, heat and chemical constituents. Within the axial zone, the heat flux from diffuse sources has been estimated to be as much as 1–10 times that from focused high-temperature venting [1,2,9]. Simple scaling of this heat flux to a mass flux, assuming a 10°C diffuse fluid temperature and a 300°C high-temperature end-member, implies that over 95% of the volume flux is from low-temperature sources within active vent fields.

Previous direct measurements of co-registered volume and heat flux at low-temperature venting sites studied areas near high-temperature sulfide vent structures [9,10] or similar locales where diffuse flow was visibly concentrated [11,12]. The measured effluent velocities in these experiments ranged from 0.5 to 140 mm/s [9,13]. These diffusely venting systems are typically believed to be composed of a mixture of high-temperature fluids and seawater that is entrained directly into the venting structure, and may be hydrologically distinct from the basaltic-hosted diffuse venting sampled in this study. A recent geochemical study of directly sampled diffuse vent fluid from the Lucky Strike hydrothermal vent field on the Mid-Atlantic Ridge showed that low-temperature venting may become hydrologically disconnected from the source high-temperature fluid [12]. In such cases the fluid may undergo a heating and cooling history that is not consistent with simple mixing of a high-temperature end-member fluid with seawater.

Co-registered measurements of effluent fluid flow and temperature have also demonstrated a strong positive correlation between the volume flux and effluent temperature at tidal or lower frequencies, with generally poor correlations at higher frequencies [9,10]. Occasional periodic flow reversals (i.e. cold seawater flowing into the crust) were also documented, and are qualitatively similar to measurements of flow reversals that have been seen in the underpressured ODP and DSDP drill holes (i.e. 1024C, 1027C and 395A) [9,14]. Tidal pumping of the seafloor is a known consequence of the dynamic water tide; but without a good estimate of permeability of the exposed crust on the seafloor, the magnitude of this periodic flushing of the upper crust has remained uncertain (see [14] for more discussion). For the pressure effect of the water tide to yield substantial periodic seawater flow into the unsedimented oceanic crust, the permeability must be sufficiently high, of order 10^{-10} m^{-2}, a value well within the range estimated for young oceanic crust [15,16]. If the occurrence of flow reversals into the exposed young ocean crust could be generalized over large areas, it would imply a zone of intense mixing within the upper 0.5 m of unsedimented oceanic crust, with major implications to geologic, hydrologic and biologic processes in the uppermost crust.

In this paper, we examine co-registered fluid flow and temperature data collected from a low-temperature diffuse vent on Axial Seamount on the Juan de Fuca Ridge in the Northeast Pacific. After describing the geologic context and background of related studies done in this area in Section 2, we describe the instrument package and sampling system in Section 3. In Sections 4 and 5, we show the volume and thermal fluxes through the sampling device and give some detail on their variations over the deployment interval. Simple modeling used in Section 6 shows that the measured diffusely venting flow through the seafloor interface in this location is overpressured with respect to what would be expected for thermal buoyancy-driven flow alone.

2. Geologic setting

Axial Seamount, the youngest member of the Cobb–Eickelberg seamount chain, is a well-studied ridge axis volcano on the central Juan de Fuca Ridge, and represents a good natural

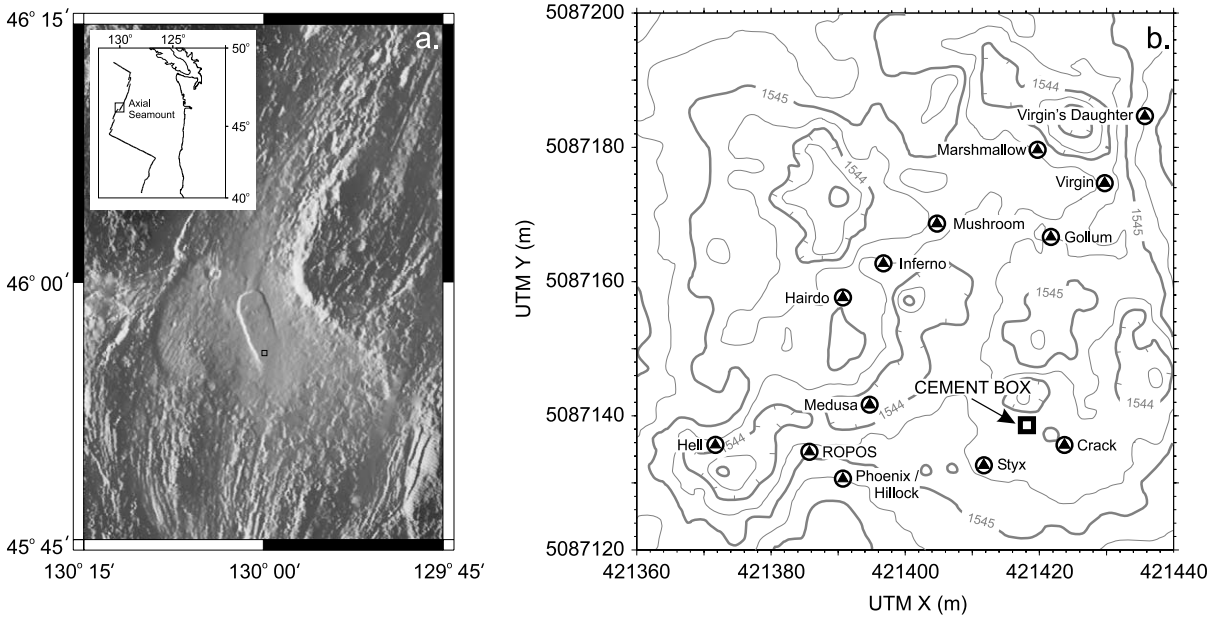

Fig. 1. Axial Seamount. (a) The instrument package was deployed in the ASHES vent field in the southwestern caldera. Lighting in the image is from the east and the depth in the image range from 1411 to 2863 m. The SeaBeam bathymetric data used in this figure were obtained from the Ridge Multibeam Synthesis Project. (b) ASHES vent field is characterized by pervasive low-temperature venting encompassing an area of roughly 200 m×1200 m. The most intense hydrothermal venting is however constrained to a 180 m×180 m region covered by smooth sheet and lobate flows. Known high-temperature vents are labeled (locations provided by R. Embley, personal communication). There is little bathymetric relief (<4 m) over this entire region of intense venting [17].

laboratory for a hydrologic study of hydrothermal systems. The caldera floor (approximately 8 km×4 km) is the locus of substantial hydrothermal venting, with several widely distributed vent fields found around the caldera rim [18]. Our monitoring package was deployed in the ASHES vent field, which is composed of approximately a dozen high-temperature (>200°C) vents and includes a large area of diffuse venting spread over approximately 0.24 km^2 (see Fig. 1a,b). The site is unusually appropriate for a long-term monitoring of fluid and temperature fluxes since the surrounding area has been well mapped and there is a long history of related fluid chemistry and geophysical measurements [19]. Ocean bottom gravity studies have shown that the seamount has an absolute porosity of approximately 38% for the upper volcanic crust, while magnetic studies indicate that the seamount has either a highly altered or a very warm (>100°C) central core [21,22]. Recent seismic tomographic mapping has confirmed the presence of a zone of partial melt approximately 1–2.5 km beneath the surface of the caldera [23].

Interestingly, prior to 1998, the area surrounding the seamount was the most tectonically active region in the Northeast Pacific detectable utilizing the US Navy's SOSSUS arrays. A volcanic eruption in January, 1998, on the southeastern caldera wall has however dramatically altered the tectonic regime, with a general paucity of earthquakes in this region following the eruption, including the Cleft segment to the south and the Co-Axial segment to the north [24]. The measurement interval for our vent monitor began in late 1998, approximately one year after the nearby eruption. The low level of local tectonic activity may have allowed the detection of a far field response to the June 8th, 1999, earthquake on the Endeavour segment, approximately 220 km to the north [25]. This earthquake, which may have been part of a larger aseismic spreading event, had significant

impact on diffuse venting at the nearby Endeavour vent fields and was recorded at several drillholes on the ridge flank as well as the sedimented Middle Valley ridge axis drillhole [26,27].

Our sampling instrument was placed in the Crack Vents region in the southwest corner of the ASHES vent field. The area is dominated by fractured ropy sheet flows. Many of the fractures (generally <5 cm in width) in this region are marked by bordering accumulations of anhydrite and have exit fluid temperatures in excess of 200°C, although there are no large anhydrite mounds or spires in this area [17]. Effluent fluid chemistries are similar to the high-temperature phase-separated (gas-enriched, low-chlorinity) fluids exiting at the anhydrite-dominated Virgin Mound vent located 40 m to the north [19]. Generally, brine-phase fluids are discharging from the high-temperature sulfide chimneys active in western part of the ASHES vent field near the caldera wall, while vapor-phase components appear to be venting as diffuse flow from the seafloor surrounding these chimneys and in anhydrite chimneys to the east. It has been proposed that the observed pattern of spatial segregation of fluid phases is due to the relative permeability variability of two-phase flow within a substrate, with brine-phase fluids confined to large flow conduits by a surrounding relative permeability barrier, and vapor-phase fluids flowing diffusely through the surrounding host rock [20].

3. Instrumentation

The seafloor boundary represents a complex and difficult location for sampling fluids, where pillow flows and fissured basalt make it difficult to obtain a reliable hydrologic seal with the seafloor. Our instrument package was designed to overcome this difficulty in order to obtain uncontaminated diffuse hydrothermal fluid samples as evidence for a microbial biosphere living within the oceanic crust [28]. Our sampling design consists of a rectangular 1 m $\times$ 1 m Teflon-lined polyethylene base surrounded by a flared-out cofferdam (Fig. 2). The cofferdam was grouted with a concrete mixture that hydrologically sealed

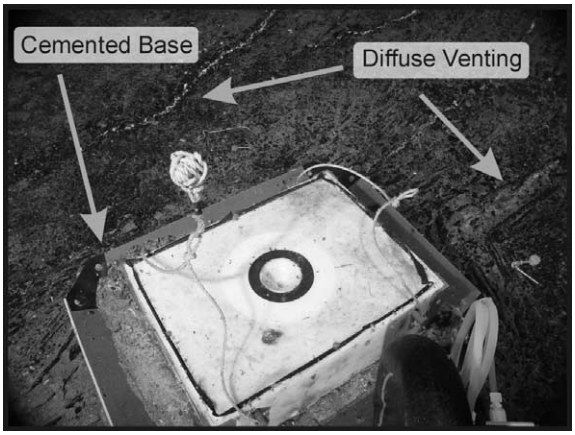

Fig. 2. The deployment is in an area of an extensive sheet flow that is fractured by a series of N–NE-trending fissures (1–3 cm in width). White stains present on some fractures are bordering accumulations of anhydrite. The instrument package was installed into the circular sampling port seen on the upper surface of the cemented base. This high-resolution digital photograph was taken by R. Embley with ROPOS during a cruise in 2002 funded by the NOAA Vents Program. Camera development was by the Canadian Scientific Support Facility and Deep Sea Power and Light.

the box to seafloor [29]. A 1 m tall instrumented column was mounted on the top of the permanently deployed base consisting of the datalogger, internal and external thermistors, a filter pack designed to measure dissolved and particulate organic carbon, and the flow sensor. The upwelling fluid was focused from the 1 m^2 of seafloor sampled by the box, through the Teflon-lined base and into a 1.27 cm diameter sampling tube where the fluid volume flux was measured. The flowmeter was a Kobold Instruments magnetic paddle wheel flow sensor (DPL-1120) modified to perform at full-ocean depths. Temperatures were recorded both at the input of the instrument port and also externally to the sampling package. All sensors initially sampled every 20.5 min during the first 21 days of the record, at which point the sample rate was slowed to one sample every 4 h for the remainder of the record.

4. Volume flux

Given that our instrument base is in contact

with an area much larger than the crack widths (1–3 cm) in the area covered by the instrument base, we can directly use our measurements of volumetric flux through the seafloor interface (see Fig. 3) and the conservation of mass equation, (i.e. $A_1 v_1 = A_2 v_2$), to calculate the Darcy velocity of the upwelling fluid within the subsurface. The specific discharge is simply the measured fluid flux rate divided by the area of the seafloor sampled:

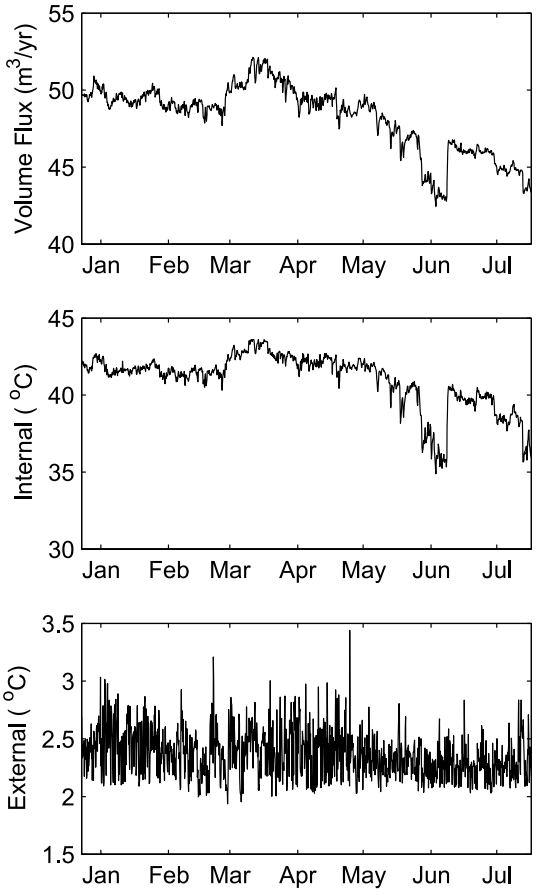

Fig. 3. Data plots showing (a) the volume flux, (b) the temperature of the effluent fluid, and (c) the temperature of the bottom water near the cement box recorded on an externally mounted thermistor. Note the rapid response that occurs within 8 h of the June 8th earthquake which occurred approximately 220 km to the north, and the possible precursor decrease in fluid flow that occurs approximately 2 weeks preceding the earthquake [25,27].

$$\bar{u} = \frac{q}{A} \tag{1}$$

The velocities measured in the instrument sampling pipe, with a diameter of 1.27 cm, ranged from 1.3 to 1.6 cm/s, yielding a specific discharge of $1.3–1.6\times10^{-6}$ m/s during the experiment interval. The total fluid flux through the 1 m^2 of seafloor sampled was 48 m^3/yr. Utilizing an idealized geometrical model for the permeability of the porous oceanic crust represented as circular tubes which form a regular cubical matrix throughout the otherwise impermeable rock matrix:

$$\bar{u} = \frac{\phi u_c}{3} \tag{2}$$

the vertical velocity of the fluid within volcanic rock matrix, u_c, can be estimated if the porosity, ϕ, is known [14,30,31]. Assuming that the effective porosity (available for fluid flow) ranges somewhere between 10% and the bulk porosity estimate of 38% obtained from seafloor gravity studies [21], and that the horizontal (non-vertical) flow within the substrate is negligible, yields vertical velocities for the fluid within cracks in the substrate of 8–30 times the Darcy velocity, or approximately 1–4 m/day.

Although these measured flow rates are low, and the tidal range in this area is of order 3×10^4 Pa [32], it is important to note that the flow out of the seafloor in this location remained positive at all times (i.e. there were no flow reversals when seawater flowed into the seafloor). Examination of shorter time intervals (see Fig. 4 for an example) indicates some consistent variance in both the internal temperature and flow measurements at roughly daily time scales. This variability may be related to poroelastic effects on the velocity of fluid through the seafloor interface, where the pore fluid pressure in the upper crustal rocks is responding to transient loading arising from the passing water tide [33]. Computing the specific discharge associated with the roughly 0.5 m^3/yr daily variability equates to a tidal volumetric flux of approximately 1.6×10^{-8} m/s. Using this Darcy velocity, a 2 m water tide amplitude and a fluid viscosity of 0.6×10^{-3} Pa s, we obtain an formation-scale effective permeability of order 10^{-12} m^2. Caution should be used in interpreting

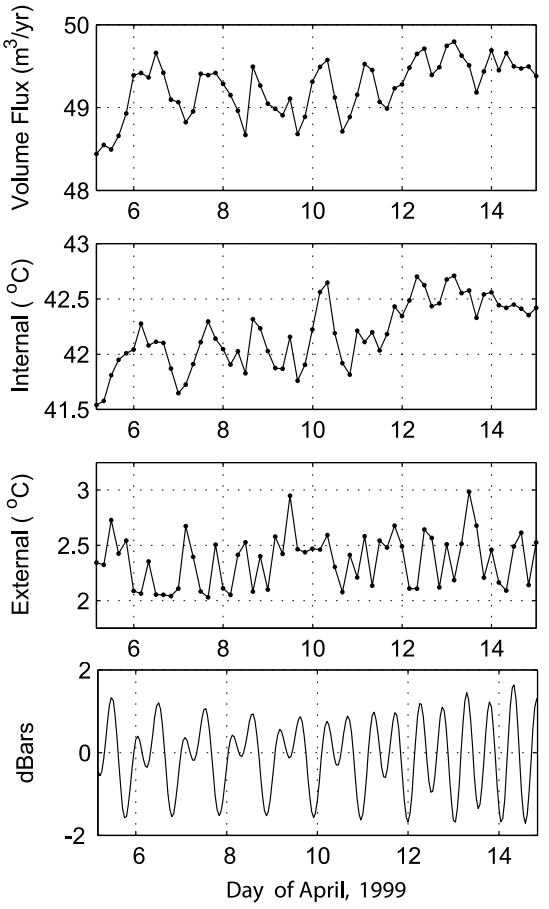

Fig. 4. Data plots showing a 10 day record of (a) volume flux, (b) temperature of the effluent fluid, (c) external thermistor recording background water temperature and (d) the modeled tidal variations utilizing a near pressure recorder [32].

this result however, since we have assumed (but not demonstrated) that the daily variations observed in the effluent velocity and temperature are a direct result of poroelastic forcing. Although the signals at periods of 24 h and greater are strongly correlated, they are not well correlated at higher frequencies. In fact, examination of the spectra at tidal frequencies indicates that neither the effluent temperature nor the velocity has a significant enhancement of energy over the 206 day deployment interval at tidal frequencies (Fig. 5). An alternative method for computing effective permeabilities is given in Section 6.

5. Thermal flux

Since we have measured both the volumetric flux and the temperature of the effluent fluid, we have also directly measured heat flux from 1 m^2 of a diffuse vent in a manner analogous to previous direct measurements of heat flux from the high-temperature point sources:

$$Q_{\mathrm{H}} = \frac{\rho_{\mathrm{f}} c_{\mathrm{p}} q (T - T_0)}{A} \tag{3}$$

where Q_{H} is the heat flux, ρ_{f} is the density of hydrothermal fluid, c_{p} is the specific heat of the fluid, q/A is the specific discharge and $(T-T_0)$ is the temperature difference between the bottom water and the hydrothermal fluid. Both the density of the hydrothermal fluid and the specific heat are functions of temperature, salinity and pressure and need to be computed at each time step. In this experiment the hydrothermal fluid density ranged from 1021.7 to 1025.3 kg/m^3, and the specific heat ranged from 3986.1 to 3992.1 J/kg/°C.

Our measured heat flux varied from 200 to 300 W/m^2 over the deployment interval, with a mean heat flux of 260 W/m^2. In 1987, diffuse heat flux was measured in this area utilizing plume measurements within the bottom boundary layer [1,34]. They obtained estimates of diffuse heat flux that ranged between 22 and 57 kW/m^2 over

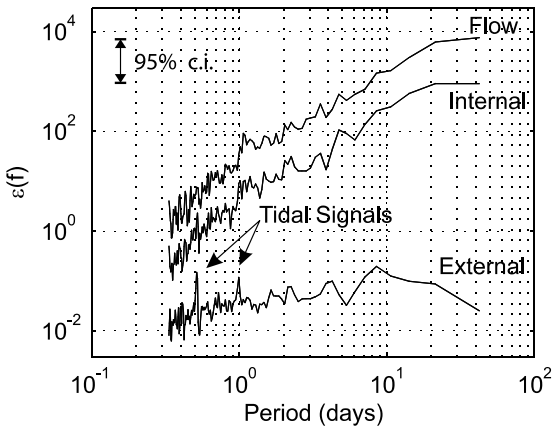

Fig. 5. Power spectral plots showing enhanced energy at tidal frequencies for the external temperature sensor and very little tidal energy in the internal flow and temperature measurements. The spectra were offset for image clarity.

nearby diffusely venting areas, and estimated that the total component of diffuse heat flux for the ASHES vent field was $15–75\times10^6$ W. This prior study did not however record a water column plume above the *crack vents* where the cement box is located, nor were they able to estimate magnitude of the diffuse heat flux for this specific site. This indicates that the area sampled by the cement box may not be characteristic of the magnitude of diffuse flow within the ASHES vent field in general, and may have broader implications. In order to obtain two orders of magnitude higher heat flux (and therefore volume flux assuming roughly equivalent effluent temperatures), significantly higher effective permeabilities would be required over relatively short spatial distances ($\sim$50 m). The disparity between these two estimates also highlights the well-known spatial and temporal variability of diffuse venting, where it is common for the temperature of the fluid exiting the crust to vary by tens of degrees over a spatial scale of decimeters and temporal scales as short as weeks.

6. Darcy flow approximation

Since we have used the daily variation in the specific discharge to estimate formation-scale permeabilities of order 10^{-12} m^2 in Section 4, it would be useful to examine whether the measured flow indeed meets the required assumptions for Darcy's law of viscous flow theory. The critical assumption in Darcy's law is that the flow within the substrate must be laminar. In order to examine this assumption, we can estimate the Reynolds number of the flow within the substrate using the formulation for flow within a pipe [35]. It has been shown experimentally for pipes and open channels that if $\mathrm{Re}\ll2300$, the flow can be considered laminar. Within an aquifer however, where the roughness of the flow path is large and the flow path very tortuous, a $\mathrm{Re}<10$ is usually required to ensure laminar flow. The Reynolds number is defined as:

$$\mathrm{Re}\equiv\frac{\rho\bar{u}D}{\mu} \tag{4}$$

where Re = Reynolds number, ρ = density of the hydrothermal fluid, $\bar{u}$ = mean velocity per unit area, D = pipe diameter and μ = fluid viscosity. Examining the Reynolds number for flow within the subsurface reservoir, utilizing the specific discharge of 1.5×10^{-6} m/s and the same fluid density and viscosity used above, we calculate that crack widths less than 1 m in width yield a $\mathrm{Re}<10$. These calculations support the expectation that subsurface flow in the crust below the cemented box should be laminar.

This laminar flow in the substrate is however focused from the 1 m^2 sampling area at the seafloor interface to a 1.27 cm sampling pipe. Computing the Reynolds number for the flow within the measurement pipe (using an equivalent volume flux as above, or $\bar{u}=1.2$ cm/s, a mean hydrothermal fluid density of 1023 kg/m^3 and $\mu=6.4\times10^{-4}$ Pa s), we get a $\mathrm{Re}\gg2300$, indicating flow within our measurement pipe should be fully turbulent. This result is supported by the spectra shown in Fig. 5, where obtaining an approximate wavenumber spectrum by scaling with the mean velocity of 1.2 cm/s yields the expected slope for turbulent flow of approximately $-5/3$. So while the subsurface flow was likely laminar (the region of interest for all the following calculations), the flow actually measured in the sampling pipe was turbulent.

Measurements of the Darcy velocity can be used to directly compute the effective permeability of the substrate using Darcy's equation of fluid flow:

$$\bar{u}=\frac{k}{\mu}\left(\frac{\mathrm{d}P}{\mathrm{d}z}-\Delta\rho g\right) \tag{5}$$

where k = permeability, μ = viscosity of the hydrothermal fluid, $\mathrm{d}P/\mathrm{d}z$ = background crustal pressure gradient, $\Delta\rho$ = density contrast between seawater and hydrothermal fluid, g = gravitational acceleration and $\bar{u}$ is the measured Darcy velocity. If fluid within the crust is hydrostatic (i.e. $\mathrm{d}P/\mathrm{d}z=0$), then Eq. 5 can be rearranged to obtain the effective permeability for each measurement interval. This yields permeability estimate ranging from 1.0×10^{-11} to 7.8×10^{-12}. This permeability is however highly correlated with the effluent fluid

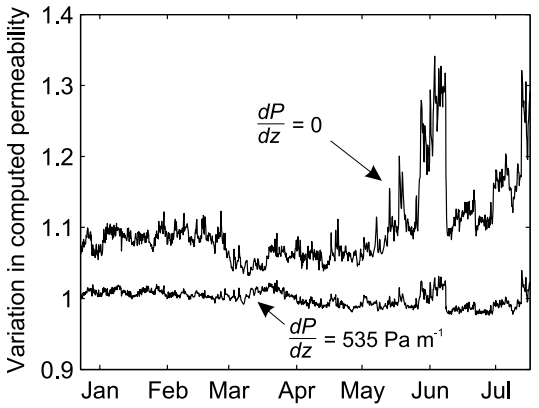

Fig. 6. Fractional variation in computed permeability found by repeatedly solving Eq. 5 and dividing the result by the median computed permeability over the deployment interval. The $dP/dz = 0$ case has been offset by 0.05 for clarity.

temperature (see Figs. 3 and 6). Relaxing the hydrostatic constraint, and instead iteratively solving Eq. 5 with the best fit determined by minimizing $\|k_i - \bar{k}\|$, we find that a mean overpressure equivalent to 535 Pa/m reduces the variance of the estimated permeability to less than 4%. This strategy produces a significant improvement during the last 90 days of deployment when there is a substantial variation in effluent temperature. The calculated overpressure would contribute approximately four times the driving force, with respect to fluid buoyancy alone, to the measured effluent velocity and would reduce the average required permeability to 1.5×10^{-12} m^2. Driving fluid flow with the overpressure alone would yield Darcy velocities of 1.25×10^{-6} m/s (or 1–3 m/day within the subsurface cracks).

It is not obvious what process would cause the calculated non-thermal overpressure in this system. The geopressuring of fluid in sedimentary basins has however been well studied and some of the most common processes associated with these systems may be analogous to the process(es) that are present in this hard-rock system: (1) aquifer head, (2) tectonic compression, (3) loading/compaction with the absence of adequate drainage systems, and/or (4) intrusion of gas or fluid phase changes. A general requirement for the anomalous subsurface pore fluid pressure is the presence of a subsurface permeability barrier that is effectively preventing, or greatly restricting, free fluid flow. It may be that the large sheet-like lava flow, upon which the sampling box is deployed, acts as an effective permeability barrier (cap rock). Other subsurface permeability barriers, including biological films or gas bubbles, cannot be excluded however.

Although the flow from the cemented box is only mildly overpressured (535 Pa/m is equivalent to transferring an additional load of 5 cm of water or 2 cm of rock to the fluid), the constant geopressure dominates the measured effluent fluxes in this low-flow hydrothermal system. It is also significant that over the course of the 206 day deployment there is no requirement for time-dependent changes in the measured effective permeability. If the upper crustal permeability is constant over this interval, it implies that the observed temporal variability in diffuse flux (mass, volume and heat) from the cemented box is a consequence of changes in: (1) the subsurface mixing, (2) the geometry of the flow paths, or (3) the addition of 'new' heat to the hydrothermal system.

7. Summary

We have measured the volumetric and heat fluxes of a diffuse vent using the direct coupling provided by an interface cemented onto the seafloor of an active volcano on a mid-ocean ridge. Volume flux of the low-temperature hydrothermal fluid is approximately 48 m^3/yr and indicates upwelling flow velocity within the subsurface at 1–4 m/day. We estimate an effective permeability of 1.5×10^{-12} m^2 for the uppermost crustal rocks of the seamount and have documented a significant, time-invariant contribution to the pressure gradient from a non-thermal process. The measured permeability is surprisingly consistent over the 206 day deployment, without any indication of significant changes in the subsurface 'plumbing' during this time. Our flux measurements are consistent with an oscillatory poroelastic-driven flow ($\sim1.5\times10^{-8}$ m/s) through the rock–water interface. This oscillatory (tidal) flow, however, constitutes less than 1% of the total flow volume from

the box, and would only represent approximately 5% of the volume flux if the overpressuring of the effluent fluid was relieved. It is likely, however, that other diffusely venting areas (with higher effective permeabilities) may be experiencing significant tidal modulation of their mass and energy fluxes on tidal time scales. Although the cemented box has allowed us to tightly characterize a small diffuse hydrothermal zone and shown the potential importance of non-thermal buoyancy terms in low-flux deep-sea hydrothermal systems, the obvious diversity of diffusely venting areas and our limited spatial sampling severely limit the broad generalization of these results.

Acknowledgements

We would like to thank Tor Bjorklund, Jim Cowen, the *Atlantis* crew and the entire *Alvin* group for so cheerfully accepting the difficult challenge that the installation of this instrument package on the seafloor proposed. We also thank Donald Janssen for access to both his expertise and also his laboratory for testing the cement mixtures, which proved critical to the success of this research. Michael Hutnak performed all the calibration, testing and instrument preparation. This research was funded by NSF Grants OCE-9911523, OCE-9618294 and BES-9729671. Carol Stein and an anonymous reviewer significantly improved the final manuscript.***[KF]***

References

[1] P.A. Rona, D.A. Trivett, Discrete and diffuse heat transfer at ASHES vent field, Axial Volcano, Juan de Fuca Ridge, Earth Planet. Sci. Lett. 109 (1992) 57–71.

[2] E.T. Baker, G.J. Massoth, S.L. Walker, R.W. Embley, A method for quantitatively estimating diffuse and discrete hydrothermal discharge, Earth Planet. Sci. Lett. 118 (1993) 235–249.

[3] D.A. Trivett, A.J. Williams III, Effluent from diffuse hydrothermal venting 2. Measurement of plumes from diffuse hydrothermal vents at the southern Juan de Fuca Ridge, J. Geophys. Res. 99 (1994) 18417–18432.

[4] J.W. Lavelle, M.A. Wetzler, E.T. Baker, R.W. Embley, Prospecting for hydrothermal vents using moored current and temperature data: Axial Volcano on the Juan de Fuca Ridge, northeast Pacific, J. Phys. Oceanogr. 31 (2001) 827–838.

[5] S.A. Little, K.D. Stolzenbach, F.J. Grassle, Tidal current effects on temperature in diffuse hydrothermal flow: Guaymas Basin, Geophys. Res. Lett. 15 (1988) 1491–1494.

[6] M.D. Rudnicki, H. Elderfield, Theory applied to the Mid-Atlantic Ridge hydrothermal plumes: the finite difference approach,, J. Volcanol. Geotherm. Res. 50 (1992) 161–172.

[7] J.W. Lavelle, M.A. Wetzler, Diffuse venting and background contributions to chemical anomalies in a neutrally buoyant ocean hydrothermal plume, J. Geophys. Res. 104 (1999) 3201–3209.

[8] M.K. Tivey, A.M. Bradley, T.M. Joyce, D. Kadko, Insights into tide-related variability at seafloor hydrothermal vents from time-series measurements, Earth Planet. Sci. Lett. 202 (2002) 693–707.

[9] A. Schultz, J.R. Delaney, R.E. McDuff, On the partitioning of heat flux between diffuse and point source seafloor venting, J. Geophys. Res. 97 (1992) 57–71.

[10] A. Schultz, P. Dickson, H. Elderfield, Temporal variations in diffuse hydrothermal flow at TAG, Geophys. Res. Lett. 23 (1996) 3471–3474.

[11] J.B. Corliss, J. Dymond, L.I. Gordon, J.M. Edmond, R.P. von Herzen, R.D. Ballard, K. Green, D. Williams, A. Brainbridge, K. Crane, T.H. van Andel, Submarine thermal springs on the Galapagos Rift, Science 203 (1979) 1073–1083.

[12] M.J. Cooper, H. Elderfield, A. Schultz, Diffuse hydrothermal fluids from Lucky Strike hydrothermal vent field: Evidence for a shallow conductively heated system, J. Geophys. Res. 105 (2000) 19369–19375.

[13] A. Schultz, H. Elderfield, Controls on the physics and chemistry of seafloor hydrothermal circulation, Phil. Trans. R. Soc. London 355 (1997) 387–425.

[14] E. Davis, K. Becker, Tidal pumping of fluid within and form the oceanic crust: new observations and opportunities for sampling the crustal hydrosphere, Earth Planet. Sci. Lett. 172 (1999) 141–149.

[15] A.T. Fisher, Permeability within basaltic oceanic crust, Rev. Geophys. 36 (1998) 143–182.

[16] A.T. Fisher, K. Becker, Channelized fluid flow in oceanic crust reconciles heat-flow and permeability data, Nature 403 (2000) 71–74.

[17] S.R. Hammond, Relationships between lava types, seafloor morphology, and the occurance of hydrothermal venting in the ASHES vent field of Axial Volcano, J. Geophys. Res. 95 (1990) 12875–12893.

[18] R.W. Embley, E.T. Baker, Interdisciplinary group explores seafloor eruption with remotely operated vehicle, EOS Trans. AGU 80 (1999) 213, 219, 222.

[19] D.A. Butterfield, G.J. Massoth, R.E. McDuff, J.E. Lupton, M.D. Lilley, Geochemistry of hydrothermal fluids from Axial Seamount Hydrothermal Emissions Study Vent Field, Juan de Fuca Ridge: Subseafloor boiling and subsequent fluid-rock interaction, J. Geophys. Res. 95 (1990) 12895–12921.

[20] C.G. Fox, Consequences of phase separation on the distribution of hydrothermal fluids at ASHES vent field, Axial Volcano, Juan de Fuca Ridge, J. Geophys. Res. 95 (1990) 12923–12926.
[21] J.A. Hildebrand, J.M. Stevenson, P.T.C. Hammer, M.A. Zumberge, R.L. Parker, A seafloor and sea surface gravity survey of Axial Volcano, J. Geophys. Res. 95 (1990) 12689–12696.
[22] M.A. Tivey, H.P. Johnson, The magnetic structure of Axial Seamount, Juan de Fuca Ridge, J. Geophys. Res. 99 (1992) 12735–12750.
[23] M. West, W. Menke, M. Tolstoy, S. Webb, R. Sohn, Magma storage beneath Axial volcano on the Juan de Fuca mid-ocean ridge, Nature 418 (2001) 833–836.
[24] R.P. Dziak, C.G. Fox, Long-term seismicity and ground deformation at Axial Volcano, Juan de Fuca Ridge, Geophys. Res. Lett. 26 (1999) 3641–3644.
[25] H.P. Johnson, R.P. Dziak, C.R. Fisher, C.G. Fox, M.J. Pruis, Earthquakes' impact on hydrothermal systems may be far-reaching, EOS Trans. AGU 82 (2001) 233–236.
[26] H.P. Johnson, M. Hutnak, R.P. Dziak, C.G. Fox, I. Urcuyo, J.P. Cowen, J. Nabelek, C. Fisher, Earthquake induced changes in a hydrothermal system on the Juan de Fuca mid-ocean ridge, Nature 407 (2000) 174–177.
[27] E.E. Davis, K. Wang, R.E. Thomson, K. Becker, J.F. Cassidy, An episode of seafloor spreading and associated plate deformation inferred from crustal fluid pressure transients, J. Geophys. Res. 106 (2001) 21953–21963.
[28] J.P. Cowen, S.J. Giovannoni, F. Kenig, H.P. Johnson, D. Butterfield, M.S. Rappé, M. Hutnak, P. Lam, Fluids from aging ocean crust that support microbial life, Science 299 (2003) 120–123.
[29] M. Hutnak, H.P. Johnson, On obtaining a hydrological seal with the sea floor: A concrete example from Axial Seamount, Ridge Events 10 (1999) 24–28.
[30] D.L. Turcotte, G. Schubert, Geodynamics: Applications of Continuum Physics to Geological Problems, John Wiley and Sons, New York, 1982, 450 pp.
[31] E.E. Davis, K. Wang, K. Becker, R.E. Thomson, Formation-scale hydraulic and mechanical properties of oceanic crust inferred from pore pressure response to periodic seafloor loading, J. Geophys. Res. 105 (2000) 13423–13435.
[32] C.G. Fox, In situ ground deformation measurements from the summit of Axial Volcano, Geophys. Res. Lett. 26 (1999) 3437–3440.
[33] K. Wang, E.E. Davis, Theory for the propagation of tidally induced pore pressure variations in layered subseafloor formations, J. Geophys. Res. 101 (1996) 11483–11495.
[34] D.A. Trivett, Effluent from diffuse hydrothermal venting 1. A simple model of plumes from diffuse hydrothermal sources, J. Geophys. Res. 99 (1994) 18403–18415.
[35] O. Reynolds, On the experimental investigation of the circumstances which determine whether the motion of water shall be direct or sinuous, and the law of resistance in parallel channels, Phil. Trans. R. Soc. London A 186 (1883) 123–164.